Investigation of Mineral Carbonation with Direct Bubbling into Concrete Sludge

Masahiro Abe, Shunsuke Tanaka, Miyuki Noguchi, and Akihiro Yamasaki*
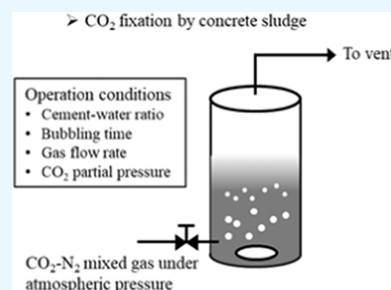
ACCESS | Metrics & More | Article Recommendations

ABSTRACT: Mineral carbonation, which is CO_2 fixation through a carbonation reaction using alkaline earth metals, is being investigated as a carbon capture and utilization method to reduce CO_2 atmospheric emissions. Concrete sludge is an alkali waste material from the concrete industry and contains abundant calcium components. We investigated the applicability of concrete sludge for mineral carbonation. In this study, gas containing CO_2 was bubbled through the model concrete sludge solution and the effects of the solid−liquid ratio, bubbling time, gas flow rate, and the partial pressure of CO_2 on the CO_2 fixation ratio and fixation rate were investigated. The CO_2 fixation ratio decreased with increasing CO_2 bubbling time, CO_2 flow rate, and CO_2 partial pressure. The CO_2 fixation rate increased with increasing CO_2 flow rate and CO_2 partial pressure. The formation of calcite, a form of calcium carbonate, was confirmed.

➤ CO_2 fixation by concrete sludge

Operation conditions
• Cement−water ratio
• Bubbling time
• Gas flow rate
• CO_2 partial pressure

To vent

CO_2-N_2 mixed gas under atmospheric pressure

1. INTRODUCTION

Global warming, caused by greenhouse gas (GHG) emissions, has become a serious problem. CO_2 makes up most to GHG emissions, and therefore has a significant impact on global warming. The 2015 Paris Agreement aimed to constrain anthropogenic warming to 1.5−2 °C by reducing CO_2 emissions,[1] and therefore a method to reduce CO_2 emissions to the atmosphere is urgently needed. One of these measures, carbon capture and storage (CCS), has been investigated to sequester of CO_2 from the atmosphere. The CCS method includes geological storage, ocean storage, and mineral carbonation. In geologic storage, CO_2 is introduced to an aquifer or coal bed layer under high pressure.[2,3] Ocean storage is generally divided into two methods: CO_2 dissolution into seawater at depths shallower than 3000 m and liquid CO_2 precipitation to the sea bottom at depths greater than 3000 m.[4,5] In these strategies, a large amount of CO_2 can be sequestered in a stable form. However, they consume energy for the separation, concentration, and liquefaction of CO_2, and therefore emit further CO_2 during the process. Furthermore, these storage methods may have additional environmental impacts such as contamination of groundwater or acidification of seawater.

We focused on mineral carbonation for CO_2 fixation in this study. Mineral carbonation fixes CO_2 as a carbonate compound by reacting CO_2 with an alkaline earth metal such as calcium or magnesium.[6] The main scheme of the mineral carbonation is expressed by

alkaline earth metal sources (Ca, Mg) + CO_2

→ carbonates ($CaCO_3$, $MgCO_3$, etc.)
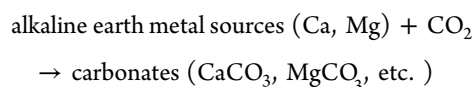
The advantage of the mineral carbonation is that the carbonation reaction proceeds spontaneously without energy supply, and carbonate salts of alkaline earth metals are highly stable with a lower Gibbs free energy. CO_2 is unlikely to be re-released into the atmosphere. The generated carbonate salts (calcium carbonate or magnesium carbonate) can be used in various industrial applications. However, a huge amount of raw materials containing calcium or magnesium should be necessary to make the mineral carbonation process a practical measure for CO_2 emission reduction. The uses of natural rocks[7−16] or waste materials[17−27] have been reported for the mineral carbonation processes. Ultramafic rocks such as olivine, serpentine, and wollastonite are potential materials for mineral carbonation with large reserves of resources. However, direct carbonation reactions of these rocks are rather slow under normal temperature and pressure conditions so that acceleration of the carbonation reaction is essential to make the process practical. Several acceleration measures have been proposed so far, which can be divided into two types: direct and indirect methods. In the direct methods, pulverized ultramafic rocks are reacted directly with gaseous CO_2 under higher-pressure and higher-temperature conditions to accelerate the carbonation reaction.[6,8−13] In the indirect methods, chemicals are used for the activation of calcium or magnesium

contained in the alkaline earth metal sources, to be dissolved into water as cations, which are more easily reacted with CO_2.[8−10,12−16] In another approach, amine compounds are used for the CO_2 absorption, which can be accelerated CO_2 dissolution without CO_2 purification and pressurization.[28−32] Both methods, however, would lead to increase in the power consumption and cost for the carbonation process. Alkaline waste materials such as fly ash, waste concrete powder, and steel making slag are also useful resources for mineral carbonation.[15−27] Mineral carbonation using alkaline waste has multiple advantages. In general, the mineralization reaction rates with wastes would be higher than those for rocks. The carbonation process can be recognized as a waste management process in addition to CO_2 emission reduction.

In this study, we used concrete sludge as an alkaline calcium source for mineral carbonation process.[33−35] Concrete sludge is waste of fresh concrete generated as excess ready-mixed concrete or washing residue of fresh concrete from concrete-using industries. A huge amount of concrete sludge has been disposed of (several million tons annually in Japan) as an industrial waste. Concrete sludge, at the present stage, is treated with acids to be neutralized, dehydrated, and disposed of in landfill. The chemical composition of concrete sludge is essentially the same as that of fresh concrete. Chemical composition of concrete sludge is reported to be water 77.1%, CaO 17.2%, SiO_3 3.2%, Fe_2O_3 1.9%, and Al_2O_3 0.6%.[34] The calcium-containing compounds in concrete sludge are clinker phases and hydrated compounds, which can be used as calcium sources for carbonation. The main components of the clinker phases are alite ($3CaO·SiO_2$), belite ($2CaO·SiO_2$), and C_3A($3CaO·Al_2O_3$), and C_4AF($4CaO·Al_2O_3·Fe_2O_3$). The hydration of cement components generates calcium hydroxide ($Ca(OH)_2$), hydrated calcium hydroxide (C−S−H such as $3CaO·2SiO_2·3H_2O$), ettringite ($3CaO·Al_2O_3·3CaSO_4·32H_2O$), and AFm phase ($Ca_4Al_2O_6(SO_4)·12H_2O$). These calcium-containing compounds would be carbonated by CO_2 to produce calcium carbonate ($CaCO_3$) and other compounds such as $3CaCO_3·2SiO_2·3H_2O$.[36−39]

The direct contact of gaseous CO_2 will proceed the carbonation reaction without acceleration measures such as high temperature, high pressure, or use of chemicals. The high activity of concrete sludge would lead to a simple and low-cost mineral carbonation process for CO_2 emission reduction. In addition, the process is a waste management process to reduce the emission of waste concrete sludge. Although the carbonation reactions of cement components used in concrete buildings have been intensively studied as a CO_2 utilization measure,[36−38,40−44] no detailed information is available in the literature on the mineral carbonation of concrete sludge by direct contact with gaseous CO_2. In this study, we studied the carbonation reaction of hydrated cement in water, a model concrete sludge, by bubbling gaseous CO_2 under various operation conditions. The effects of operation conditions such as solid (cement)/liquid (water) S/L ratio, bubbling time, CO_2 flow rate, CO_2 partial pressure (balanced with nitrogen) on the CO_2 fixation performances, CO_2 fixation rate, and CO_2 fixation ratio were investigated. Based on the experimental results, the mineral carbonation process of concrete sludge was evaluated in terms of the process feasibility as a CO_2 emission reduction measure.

2. MATERIALS AND METHODS

Figure 1 shows a schematic drawing for the experimental apparatus. The reaction vessel is made of acrylic resin (height
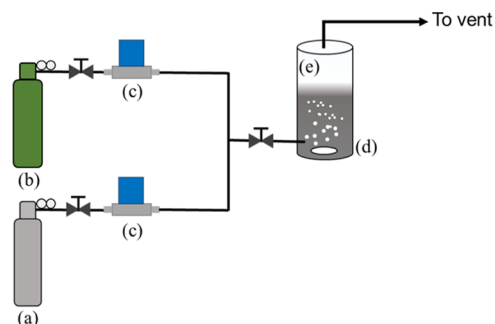
Figure 1. Schematic drawing for the experimental apparatus: (a) nitrogen gas cylinder, (b) carbon dioxide cylinder, (c) mass flow controller, (d) magnetic stirrer, and (e) reaction vessel.

400 mm, inner diameter 60 mm). A mixture of commercial Portland cement (Taiheiyo Cement Co., Tokyo) and deionized water was used as a model concrete sludge. The ratio of the cement and water (solid−liquid S/L ratio) was changed in the range of 1:100 to 1:20 (solid/liquid ratio, S/L = 0.01−0.05). The mixture was introduced to the vessel and stirred with a magnetic stirrer at 300 rpm to be hydrated for a given period without gas bubbling. The prehydration time was fixed at 60 min. After prehydration, the feed gas was supplied from a gas cylinder to the vessel from the bottom through a plastic tube (inner diameter 5 mm) to be reacted with the model concrete sludge while ascending through the vessel. The gas was then discharged to the atmosphere. The CO_2 partial pressure of the feed gas was changed from 0.05 (5 mol %) to 1 atm (100 mol %) balanced with nitrogen, simulating the composition of the various CO_2 sources. The flow rate of the feed gas was changed in the range of 100−500 mL/min controlled by a mass flow controller. The gas bubbling was carried out for 60−480 min. All of the experiments were carried out at room temperature and atmospheric pressure. Each experiment was performed at least three times under the same condition to confirm the reproducibility. The pH of the solution was measured with a pH meter. The liquid sample was filtrated by a syringe filter (0.025 μm pore size), and the calcium concentration was measured with an inductively coupled plasma-atomic emission spectrophotometer (Thermo Fisher Scientific, ICPA-6000, CA). After completion of bubbling, the sample mixture was filtered, and the solid residue was dried in a thermostatic oven at 100 °C for 24 h. The dried solid residue was analyzed by X-ray diffraction (XRD; Rigaku, Ultima IV, Tokyo, Japan). The content of calcium carbonate in the dried solid residue was determined by a thermogravimetric analyzer (TGA, Shimadzu DTG-60H, Kyoto, Japan), and the amount of CO_2 fixation as $CaCO_3$ was calculated as follows. The sample was heated from room temperature to 1000 °C at 10 °C/min. The weight loss at the temperature range between 600 and 900 °C was attributed to the decomposition of $CaCO_3$ in the sample. Based on the results, the CO_2 fixation ratio (mol %), CO_2 fixation rate, and calcium conversion were calculated by the following equations.

CO_2 fixation ratio [mol %]

$$= \frac{\text{CO}_2 \text{ in calcium carbonate [mol]}}{\text{CO}_2 \text{ provided in the system [mol]}} \times 100 \ [\%]$$
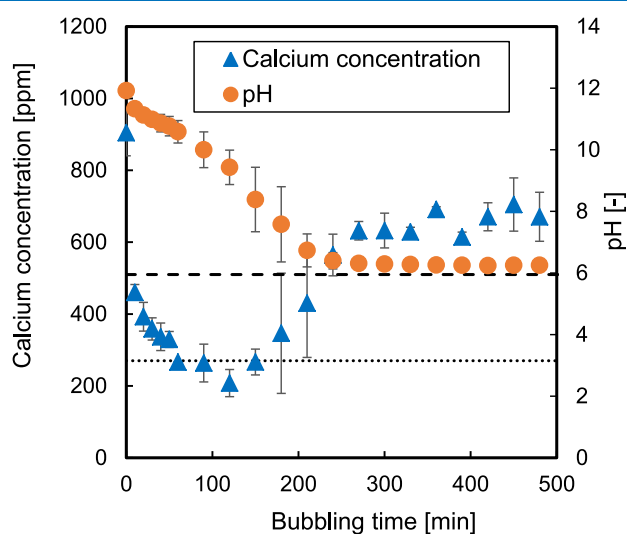
CO_2 fixation rate [mmol·(min·g − cement)$^{-1}$]

$$= \frac{\text{CO}_2 \text{ fixed as calcium carbonate [mmol]}}{\text{cement in feed [g]} \times \text{bubbling time [min]}}$$

calcium conversion [mol %]

$$= \frac{\text{calcium in CaCO}_3}{\text{calcium in cement feed}} \times 100 \ [\%]$$
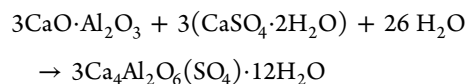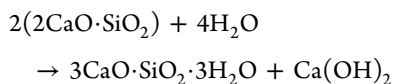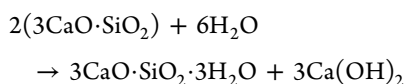
3. RESULTS AND DISCUSSION

3.1. Time Variation of Calcium Concentration and pH under CO_2 Bubbling. Figure 2 shows the changes in calcium


Figure 2. Changes in calcium concentration and pH over time (flow rate 300 mL/L, S/L ratio 0.05 g/g, CO_2 partial pressure 1.0 atm). The dotted line indicates the equilibrium calcium concentration, and the dashed line indicates the equilibrium pH. Error bars are drawn based on the repeated experiments.

concentration and pH over time under operation conditions with the CO_2 flow rate of 300 mL/min, S/L ratio of 0.05 g/g, and CO_2 partial pressure of 1.0 atm. Error bars shown are evaluated based on the repeated experiments under the same conditions. The prehydration time was 60 min, the initial pH after prehydration was about 12, and the calcium concentration was about 1000 ppm. The hydration reactions of cement components, namely, carbonation of clinker phases, alite C_3S (Ca_3SiO_5, about 55 wt %), belite C_2S (Ca_2SiO_4, about 20 wt %), and C_3A, are as follows[40,41]

$$2(3\text{CaO·SiO}_2) + 6\text{H}_2\text{O}$$
$$\rightarrow 3\text{CaO·SiO}_2\text{·}3\text{H}_2\text{O} + 3\text{Ca(OH)}_2$$

$$2(2\text{CaO·SiO}_2) + 4\text{H}_2\text{O}$$
$$\rightarrow 3\text{CaO·SiO}_2\text{·}3\text{H}_2\text{O} + \text{Ca(OH)}_2$$

$$3\text{CaO·Al}_2\text{O}_3 + 3(\text{CaSO}_4\text{·}2\text{H}_2\text{O}) + 26\ \text{H}_2\text{O}$$
$$\rightarrow 3\text{Ca}_4\text{Al}_2\text{O}_6(\text{SO}_4)\text{·}12\text{H}_2\text{O}$$

By the hydration process, calcium hydroxide is produced and dissolved in water. Based on the solubility calcium hydroxide (0.16 g/L at 20 °C), the equilibrium calcium concentration is 948 ppm-Ca and the equilibrium pH = 11.63 for saturated solution of Ca(OH)_2. The observed initial concentration of calcium in the slurry of hydrated cement before CO_2 bubbling (~1000 ppm) corresponds to the solubility of calcium hydroxide, which indicates that the dissolved calcium ions are mainly originated from calcium hydroxide.

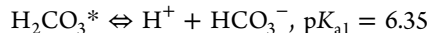$$\text{Ca(OH)}_2 \rightarrow \text{Ca}^{2+} + 2\text{OH}^-$$
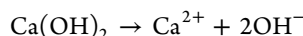
After bubbling started, the calcium concentration dropped sharply and kept constant at about 270 ppm between 60 and 150 min after the start of bubbling. Then, the calcium concentration increased and reached 600 ppm after 300 min. After that, the calcium concentration was almost unchanged. After bubbling started, the pH gradually decreased from 12 to 6 after 250 min; then, the pH was almost constant at about 6.

The decrease in the dissolved calcium concentration by the CO_2 bubbling can be attributed to the formation of calcium carbonate by the following reactions. The CO_2 in the feed gas dissolved into aqueous phase and hydrated to form H_2CO_3^*.

$$\text{CO}_2(\text{g}) + \text{H}_2\text{O} \Leftrightarrow \text{H}_2\text{CO}_3^*, \ \text{p}K_H = 1.47\ \text{atm}^{-1}$$

The hydrated CO_2 will be dissociated through the following steps

$$\text{H}_2\text{CO}_3^* \Leftrightarrow \text{H}^+ + \text{HCO}_3^-, \ \text{p}K_{a1} = 6.35$$

$$\text{HCO}_3^- \Leftrightarrow \text{H}^+ + \text{CO}_3^{2-}, \ \text{p}K_{a2} = 10.33$$

The proportion of $[\text{HCO}_3^-]$ to $[\text{CO}_3^{2-}]$ depends on pH, consequently the partial pressure of CO_2, namely, p_{CO_2} in the gas phase. When calcium ions dissolve in water, the precipitation of calcium carbonate takes place by the following reaction
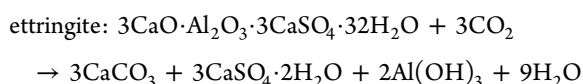
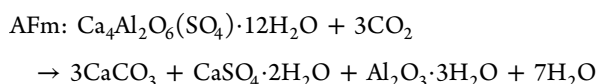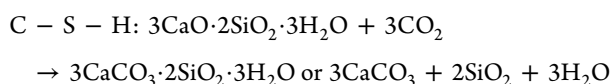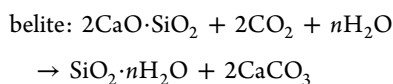$$\text{Ca}^{2+} + \text{CO}_3^{2-} \rightarrow \text{CaCO}_3 \downarrow, \ K_{SP} = 3.8 \times 10^{-9} \ (\text{mol/L})^2$$
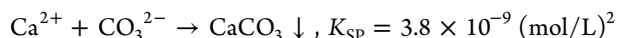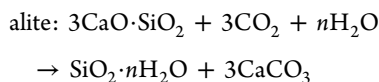
Carbonate ions would be continuously provided by the bubbling of CO_2-containing feed gas, and calcium ions would be provided into aqueous phase from the calcium hydrate in the hydrated cement. Thus, calcium carbonate would be continuously generated by the bubbling of CO_2 until all of the calcium hydroxide in the hydrate cement dissolved.

Based on the thermodynamic calculation for $p_{\text{CO}_2} = 1.0$ atm, the equilibrium calcium concentration is 270 ppm based on the solubility product of calcite ($K_{SP} = 3.8 \times 10^{-9} \ (\text{mol/L})^2$) at 25 °C, which is close to the concentration observed 60−150 min. On the other hand, the calculated pH was 5.95, which agreed with the observed pH being constant after 250 min. This result indicates that calcium carbonate was formed and precipitated at the early stage up to 150 min corresponding to the equilibrium condition. However, at a later stage, the phase of calcium carbonate would be converted with higher solubility, such as amorphous calcium carbonate ($K_{SP} = $ ~10^{-6} $(\text{mol/L})^2$).[42−44] This is the reason for the higher calcium concentration (600 ppm) after 300 min bubbling. The formation of amorphous calcium carbonate can be partially

confirmed by the weight loss of the solid sample for TG in the lower-temperature range.

Besides the carbonation of dissolved calcium ions, cement clinker phases (alite and belite) and hydration products such as calcium silicate hydrate, AFm, and ettringite other than calcium hydroxide will react with CO_2 to form calcium carbonate as follows[36,38−41]

alite: $3CaO \cdot SiO_2 + 3CO_2 + nH_2O$

$\rightarrow SiO_2 \cdot nH_2O + 3CaCO_3$

belite: $2CaO \cdot SiO_2 + 2CO_2 + nH_2O$

$\rightarrow SiO_2 \cdot nH_2O + 2CaCO_3$

$C - S - H: 3CaO \cdot 2SiO_2 \cdot 3H_2O + 3CO_2$

$\rightarrow 3CaCO_3 \cdot 2SiO_2 \cdot 3H_2O$ or $3CaCO_3 + 2SiO_2 + 3H_2O$

AFm: $Ca_4Al_2O_6(SO_4) \cdot 12H_2O + 3CO_2$

$\rightarrow 3CaCO_3 + CaSO_4 \cdot 2H_2O + Al_2O_3 \cdot 3H_2O + 7H_2O$

ettringite: $3CaO \cdot Al_2O_3 \cdot 3CaSO_4 \cdot 32H_2O + 3CO_2$

$\rightarrow 3CaCO_3 + 3CaSO_4 \cdot 2H_2O + 2Al(OH)_3 + 9H_2O$

The main product of the carbonation process is calcium carbonate.

The CO_2 fixation ratio was 2.7 mol % and the CO_2 fixation rate was 0.016 mmol/(min·g) after 480 min bubbling. These results indicate that a very small portion of calcium in cement was used for carbonation reaction; more than 97% of calcium in cement was unused for carbonation. Also, the proportion of CO_2 reacted (0.32 mmol/min) against supplied (12.3 mmol/min) is 2.6%. These CO_2 fixation performances have a lot of room for improvement through controlling the operation parameters. On the other hand, the conversion of calcium in the feed cement to calcium carbonate was 67.5% after 480 min of bubbling. Note that the conversion is calculated based on the amount of calcium carbonate produced.

Figure 3 shows the XRD pattern of the solid residue after carbonation for 480 min and that of the raw Portland cement
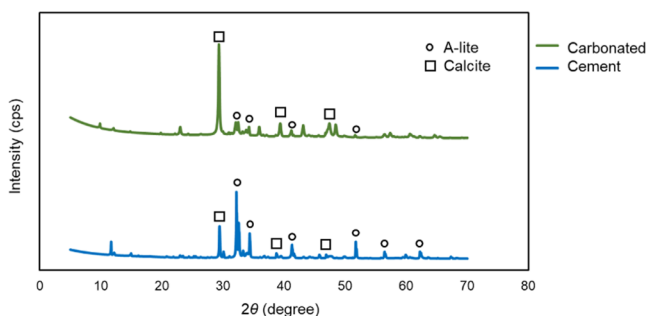

Figure 3. XRD pattern of the solid residue after carbonation for 60 min and of the raw Portland cement used in this study.

used in this study. The intensity of assigned calcium carbonate, calcite, is found to increase after carbonation reaction. Thus, the main product of the carbonation process is calcite, the most stable phase of calcium carbonate under ambient conditions. Note that amorphous carbonate cannot be detected by XRD.

3.2. Effect of Solid−Liquid (S/L) Ratio. The solid−liquid (S/L) ratio of concrete sludge depends on the source; concrete sludge with higher S/L ratios are generated from excess fresh concrete and that with lower S/L ratios are generated as washing residue. The CO_2 fixation performance should depend on the S/L ratio.

Figure 4 shows the CO_2 fixation ratio and the CO_2 fixation rate for various S/L ratios. For all of the runs, bubbling time,
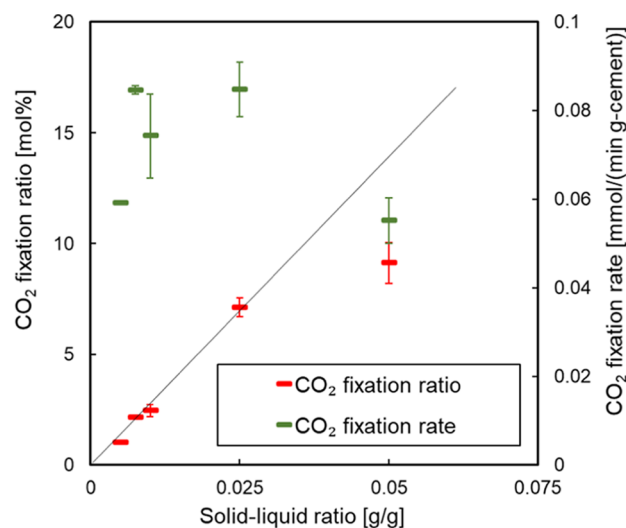
Figure 4. Influence of the S/L ratio on the fixation rate and fixation ratio. Bubbling time, 60 min; flow rate, 300 mL/L; CO_2 partial pressure, 1 atm.
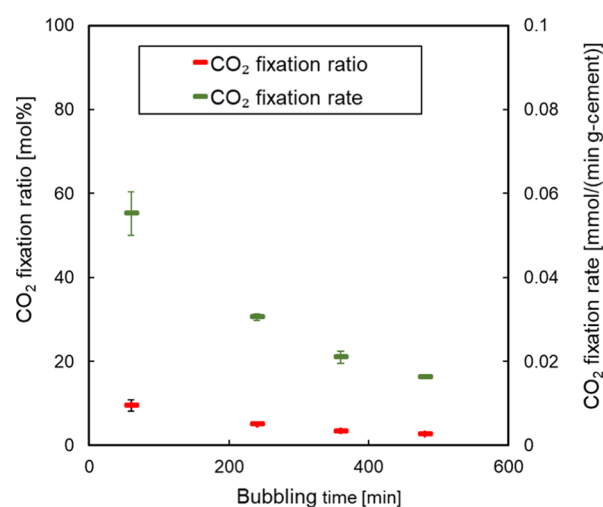
flow rate, and partial pressure of CO_2 were fixed at 60 min, 300 mL/min, and 1.0 atm, respectively. The bubbling time was fixed at 60 min because the calcium concentration would increase after that due to the dissolution of calcium carbonate once precipitated as shown in Figure 2.

The CO_2 fixation ratio increased almost linearly with increasing S/L ratio up to 0.025 and slightly leveled off after that. This is because a larger amount of calcium is available for CO_2 fixation for the higher S/L ratio conditions. This result is consistent with that the CO_2 fixation rate, i.e., the amount of CO_2 fixed per unit amount of cement is almost independent of the S/L ratio for the S/L ratio except the highest S/L of 0.05. For the S/L ratio of 0.05, an excess amount of concrete sludge was fed, which would decrease the portion of calcium used for the carbonation.

3.3. Effect of Bubbling Time. Next, we investigated the effect of the bubbling time on the CO_2 fixation performances. Figure 5 shows the effects of bubbling time on the CO_2 fixation ratio and CO_2 fixation rate at the fixed S/L ratio of 0.05 g/g. Flow rate and partial pressure of CO_2 were constant at 300 mL/min and 1.0 atm, respectively. The CO_2 fixation ratio as well as the CO_2 fixation rate decreased with increasing bubbling time, and the highest CO_2 fixation ratio was 9.55 mol % and the highest CO_2 fixation rate was 0.055 mmol/(min·g) at 60 min of the bubbling time. The longer bubbling time reduced both the fixation ratio and the fixation rate due to the decrease in the amount of calcium available for the fixation at the later stage. Note that for the fixed S/L ratio, the calcium provided from the hydrate cement is constant and determined by the initial amount of cement.

3.4. Effect of CO_2 Flow Rate. For the practical operation, the CO_2 flow rate is an important factor affecting the CO_2

Figure 5. Influence of bubbling time on the fixation rate and fixation ratio. S/L ratio, 0.05 g/g; flow rate, 300 mL/min; CO_2 partial pressure, 1.0 atm.

fixation performances. Figure 6 shows the effect of CO_2 flow rate on the CO_2 fixation ratio and the CO_2 fixation rate under the S/L ratio of 0.05 g/g, bubbling time of 60 min, and CO_2 partial pressure of 1 atm.
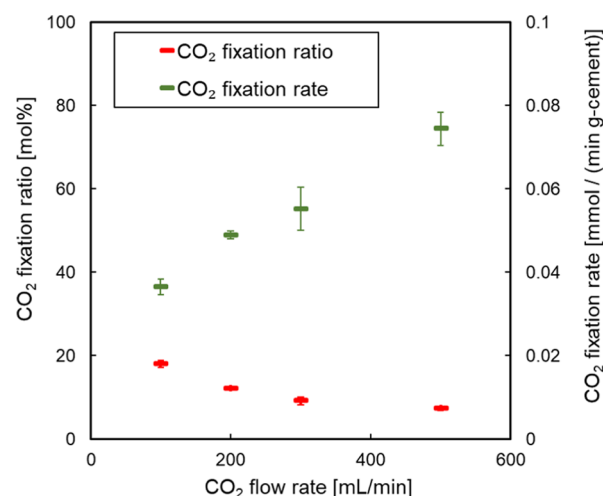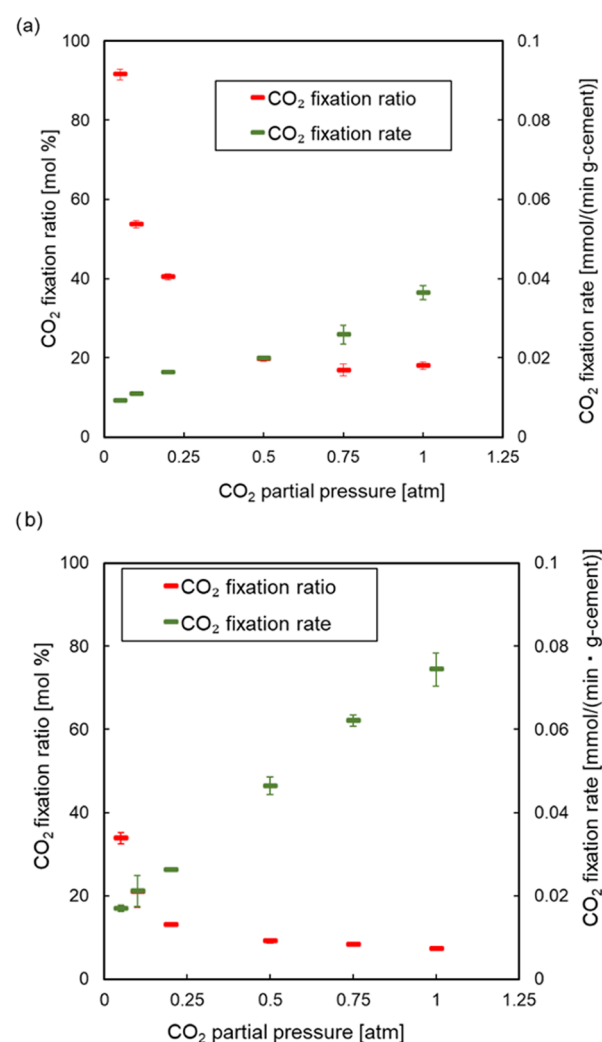

Figure 6. Influence of CO_2 flow rate on the fixation rate and fixation ratio. S/L ratio, 0.05 g/g; bubbling time, 60 min; CO_2 partial pressure, 1 atm.

The CO_2 fixation ratio decreased with increasing CO_2 flow rate, while the CO_2 fixation rate increased with increasing CO_2 flow rate. The higher CO_2 flow rate would increase the portion of supplied CO_2 that discharged from without reaction in the vessel. This is the reason for the decrease in the fixation ratio with increasing flow rate. On the other hand, the higher flow rate would facilitate the mass transfer rate, presumably increase the dissolution rate of CO_2 into the aqueous phase, and the fixation rate increased with increasing CO_2 flow rate.

3.5. Effect of CO_2 Partial Pressure. Because the CO_2 partial pressure of the target flue gas depends on the source, the effect of CO_2 pressure on the CO_2 fixation performances should be clarified.

Figure 7a,b shows the effects of the CO_2 partial pressure on the CO_2 fixation rate and the CO_2 fixation ratio under the

Figure 7. Influence of CO_2 partial pressure on the CO_2 fixation rate and fixation ratio (S/L ratio, 0.05 g/g; bubbling time, 60 min; flow rate (a) 100 mL/min and (b) 500 mL/min).

conditions of the S/L ratio at 0.05 g/g, bubbling time at 60 min, and CO_2 flow rate at 100 mL/min (a) and 500 mL/min (b). For the CO_2 flow rate at 100 mL/min, the increasing CO_2 partial pressure resulted in increasing CO_2 fixation rate almost linearly. On the other hand, the increasing CO_2 flow rate resulted in a rapid decrease in the CO_2 fixation rate at a lower CO_2 pressure, and almost unchanged at a CO_2 pressure higher than 0.5 atm. The highest CO_2 fixation ratio was 91 mol % at 0.05 atm, and the highest CO_2 fixation rate was 0.074 mmol/(min·g) at 1.0 atm for the flow rate at 500 mL/min. For the CO_2 flow rate at 500 mL/min, the increasing CO_2 partial pressure resulted in an increase in the CO_2 fixation rate more eminently, and the effect of the CO_2 partial pressure on the CO_2 fixation ratio was less remarkable than the case with a lower flow rate at 100 mL/min. The increase in the CO_2 fixation rate with increasing CO_2 partial pressure would be due to the higher CO_2 concentration dissolved in water. This effect would be accelerated by the higher flow rate due to an increase in the dissolution and mass transfer rate of CO_2. The lower CO_2 fixation ratio at higher CO_2 partial pressure is because the excess amount of CO_2 would be supplied to the system compared with the calcium available in the system under the fixed S/L ratio.

The experimental results obtained in this study are summarized in Table 1. The CO_2 fixation ratio decreased

Table 1. Summary of the Effects of Operation Parameters on the CO_2 Fixation Performances

parameter to be increased	range tested	CO_2 fixation ratio	CO_2 fixation rate
S/L ratio	0.005−0.05 cement/water	increased	not much affected, except high S/L
CO_2 bubbling time	60−480 min	decreased	decreased
CO_2 flow rate	100−500 mL/min	decreased	increased
CO_2 partial pressure	0.05−1.0 atm	decreased	increased

with increasing CO_2 bubbling time, CO_2 flow rate, and CO_2 partial pressure. These results indicate that when a larger amount of CO_2 is supplied to the reaction system, the smaller portion of supplied CO_2 will be used for the carbonation reaction. On the other hand, the CO_2 fixation rate increased with increasing CO_2 flow rate and CO_2 partial pressure. This trend can be explained by the increase in the mass transfer rate of CO_2 dissolution and increase in the concentration of dissolved CO_2 in water by increasing the CO_2 flow rate and CO_2 partial pressure. The decrease in the CO_2 fixation rate with increasing CO_2 bubbling time is due to the depletion of available calcium for carbonation reaction under a fixed calcium amount, i.e, a fixed S/L ratio. When the CO_2 supply is fixed, the higher amount of cement (higher S/L ratio) resulted in a higher CO_2 fixation ratio because a greater amount of calcium is available for carbonation. However, the CO_2 fixation rate seems to be mainly controlled by the CO_2 supply, which was found to be not much affected by the S/L ratio.

The highest CO_2 fixation ratio was 91.5% that was obtained for the following conditions: CO_2 partial pressure, 0.05 atm; S/L ratio, 0.05; CO_2 flow rate, 100 mL/min; and bubbling time, 60 min, as shown in Table 2. The CO_2 fixation rate under these conditions was 0.0092 mmol/(min·g). In this case, the calcium conversion was 4.76%. On the other hand, the highest CO_2 fixation rate was 0.085 mmol/(min·g), which was obtained for the conditions of CO_2 partial pressure, 1.0 atm; S/L ratio, 0.0075 or 0.025; CO_2 flow rate, 300 mL/min; and

Table 2. Summary of the Highest CO_2 Fixation Performances and Operation Parameters

parameter	range tested	highest fixation ratio (%)	highest fixation rate (mmol/(min·g))
S/L ratio (cement/water)	0.005−0.05	9.1% at 0.05	0.085 at 0.025 and 0.0075
CO_2 bubbling time (min)	60−480	9.6% at 60 min	0.055 at 60 min
CO_2 flow rate (mL/min)	100−500	18.0% at 100 mL/min	0.074 at 500 mL/min
CO_2 partial pressure (atm) for 100 mL/min	0.05−1.0	91.5% at 0.05 atm	0.036 at 1 atm
CO_2 partial pressure (atm) for 500 mL/min	0.05−1.0	33.8% at 0.05 atm	0.074 at 1 atm

bubbling time, 60 min. The CO_2 fixation ratios under these conditions were 2.2 and 7.2%, respectively, for the S/L ratios of 0.0075 and 0.025. The calcium conversions were 43.8 and 43.9% for S/L = 0.0075 and 0.025, respectively.

From the viewpoint of the process design, when a higher CO_2 fixation ratio is required, higher S/L ratio, lower bubbling rate, and shorter bubbling time are favorable. On the contrary, when a higher CO_2 fixation ratio is required, which leads to a higher-ratio cement used for carbonation, shorter bubbling time and higher bubbling rate are favorable. The CO_2 partial pressure in the feed gas affects the CO_2 fixation performances, but that is a given condition depending on the CO_2 emission source and uncontrollable. The bubbling method of CO_2 would affect the dissolution rate of CO_2 into the water phase; the use of a gas diffuser would increase the gas dissolution rate of CO_2 into the water phase.

4. CONCLUSIONS

Mineral carbonation by bubbling to model concrete sludge was investigated under various experimental conditions. The CO_2 fixation ratio decreased with increasing CO_2 bubbling time, CO_2 flow rate, and CO_2 partial pressure. The CO_2 fixation rate increased with increasing CO_2 flow rate and CO_2 partial pressure. The highest CO_2 fixation ratio of 91.5% was obtained at a CO_2 partial pressure of 0.05 atm, S/L ratio of 0.05, CO_2 flow rate of 100 mL/min, and bubbling time of 60 min, with the CO_2 fixation rate of 0.0092 mmol/(min·g·cement). The highest CO_2 fixation rate of 0.085 mmol/(min·g) was obtained at a CO_2 partial pressure of 1.0 atm, S/L ratio of 0.0075 or 0.025, CO_2 flow rate of 300 mL/min, and bubbling time of 60 min. The CO_2 fixation ratio under these conditions were 2.2 and 7.2%, respectively, for the S/L ratios of 0.0075 and 0.025. The formation of calcite, a form of calcium carbonate, was confirmed.

■ AUTHOR INFORMATION

Corresponding Author

   Akihiro Yamasaki − *Department of Materials and Life Science, Faculty of Science and Technology, Seikei University, Tokyo 180-8633, Japan*; Phone: +81-422-37-3887; Email: akihiro@st.seikei.ac.jp

Authors

   Masahiro Abe − *Department of Materials and Life Science, Faculty of Science and Technology, Seikei University, Tokyo 180-8633, Japan*; ⓘ orcid.org/0000-0002-4100-9031

   Shunsuke Tanaka − *Department of Materials and Life Science, Faculty of Science and Technology, Seikei University, Tokyo 180-8633, Japan*

   Miyuki Noguchi − *Department of Materials and Life Science, Faculty of Science and Technology, Seikei University, Tokyo 180-8633, Japan*

Complete contact information is available at:
https://pubs.acs.org/10.1021/acsomega.0c04758

Notes

The authors declare no competing financial interest.

■ REFERENCES

(1) United Nations Framework Convention on Climate Change. *Report of the Conference of the Parties on Its Twenty-First Session, held in Paris from 30 November to 13 December 2015*; UNFCCC: Geneva, 2016.

(2) Diao, Y.; Zhang, S.; Wang, Y.; Li, X.; Cao, H. Short-term safety risk assessment of CO_2 geological storage projects in deep saline aquifers using the Shenua CCS demonstration project as a case study. *Environ. Earth Sci.* **2015**, *73*, 7571−7586.

(3) Jeon, P. R.; Kim, D.-W.; Lee, C.-H. Dissolution and reaction in a CO_2-brine-clay mineral particle system under geological CO_2 sequestration from subcritical to supercritical conditions. *Chem. Eng. J.* **2018**, *347*, 1−11.

(4) Ödalen, M.; Nycander, J.; Oliver, K. I. C.; Brodeau, L.; Ridgwell, A. The influence of the ocean circulation state on ocean carbon storage and CO_2 drawdown potential in an Earth system model. *Biogeosciences* **2018**, *15*, 1367−1393.

(5) Seo, S.; Mastiani, M.; Hafez, M.; Kunkel, G.; Asfour, C. G.; Garcia-Ocampo, K. I.; Linares, N.; Saldana, C.; Yang, K.; Kim, M. Injection of in-situ generated CO_2 microbubbles into deep saline aquifers for enhanced carbon sequestration. *Int. J. Greenhouse Gas Control* **2019**, *83*, 256−264.

(6) Oelkers, E. H.; Gislason, S. R.; Matter, J. Mineral carbonation of CO_2. *Elements* **2008**, *4*, 333−337.

(7) Abe, Y.; Iizuka, A.; Nagasawa, H.; Yamasaki, A.; Yanagisawa, Y. Dissolution rates of alkaline rocks by carbonic acid: Influence of solid/liquid ratio, temperature, and CO_2 pressure. *Chem. Eng. Res. Des.* **2013**, *91*, 933−941.

(8) Gerdemann, S. J.; O'Connor, W. K.; Dahlin, D. C.; Penner, L. R.; Rush, H. Ex Situ Aqueous Mineral Carbonation. *Environ. Sci. Technol.* **2007**, *41*, 2587−2593.

(9) Park, A.-H. A.; Jadhav, R.; Fan, L.-S. CO_2 mineral sequestration: chemically enhanced aqueous carbonation of serpentine. *Can. J. Chem. Eng.* **2003**, *81*, 885−890.

(10) Sanna, A.; Wang, X.; Lacinska, A.; Styles, M.; Paulson, T.; Maroto-Valer, M. M. Enhancing Mg extraction from lizardite-rich serpentine for CO_2 mineral sequestration. *Miner. Eng.* **2013**, *49*, 135−144.

(11) Huijgen, W. J. J.; Witkamp, G. J.; Comans, R. N. J. Mechanisms aqueous wollastonite carbonation as possible CO_2 sequestration process. *Chem. Eng. Sci.* **2006**, *61*, 4242−4251.

(12) Wang, F.; Dreisinger, D.; Jarvis, M.; Hitchins, T. Kinetics and mechanism of mineral carbonation of olivine for CO_2 sequestration. *Miner. Eng.* **2019**, *131*, 185−197.

(13) Li, J.; Jacobs, A. D.; Hitch, M. Direct aqueous carbonation on olivine at a CO_2 partial pressure of 6.5 MPa. *Energy* **2019**, *173*, 902−910.

(14) Power, I. M.; Harrison, A. L.; Dipple, G. M. Accelerating mineral carbonation using carbonic anhydrase. *Environ. Sci. Technol.* **2016**, *50*, 2610−2618.

(15) Gadikota, G.; Matter, J.; Kelemen, P.; Park, A.-H. A. Chemical and morphological changes during olivine carbonation for CO_2 storage in the presence of NaCl and $NaHCO_3$. *Phys. Chem. Chem. Phys.* **2014**, *16*, 4679−4693.

(16) Gadikota, G.; Matter, J.; Kelemen, P.; Park, A.-H. A.; et al. Elucidating the differences in the carbon mineralization behaviors of calcium and magnesium bearing alumino-silicates and magnesium silicates for CO_2 storage. *Fuel* **2020**, *277*, No. 117900.

(17) De Ceukelaire, L.; Van Nieuwenburg, D. Accelerated carbonation of a blast-furnace cement concrete. *Cem. Concr. Res.* **1993**, *23*, 442−452.

(18) Eloneva, S.; Teir, S.; Salminen, J.; Forgelholm, C. J.; Zevenhoven, R. Fixation of CO_2 by carbonating calcium derived from blast furnace slag. *Energy* **2008**, *33*, 1461−1467.

(19) Huijgen, W. J. J.; Witkamp, G. J.; Comans, R. N. J. Mineral CO_2 sequestration by steel slag carbonation. *Environ. Sci. Technol.* **2005**, *39*, 9676−9682.

(20) Bao, W.; Li, H.; Zhang, Y. Selective leaching of steelmaking slag for indirect CO_2 mineral sequestration. *Ind. Eng. Chem. Res.* **2010**, *49*, 2055−2063.

(21) Chang, E.-E.; Pan, S.-Y.; Chen, Y.-H.; Chu, H.-W.; Wang, C.-F.; Chiang, P.-C. CO_2 sequestration by carbonation of steelmaking slags in an autoclave reactor. *J. Hazard. Mater.* **2011**, *195*, 107−114.

(22) He, L.; Yu, D.; Wu, J.; Xu, M.; et al. A novel method for CO_2 sequestration via indirect carbonation of coal fly ash. *Ind. Eng. Chem. Res.* **2013**, *52*, 15138−15145.

(23) Ben Ghacham, A.; Cecchi, E.; Cecchi, E.; Blais, J.-F.; Mercier, G. CO_2 sequestration using waste concrete and anorthosite tailings by direct mineral carbonation in gas−solid−liquid and gas−solid routes. *J. Environ. Manage.* **2015**, *163*, 70−77.

(24) Ben Ghacham, A.; Pasquier, L. C.; Cecchi, E.; Blais, J. F.; Mercier, G. Valorization of waste concrete through CO_2 mineral carbonation: Optimizing parameters and improving reactivity using concrete separation. *J. Cleaner Prod.* **2017**, *166*, 869−878.

(25) Abbaspour, A.; Tanyu, B. F. CO_2 sequestration by carbonation processes of rubblized concrete at standard conditions and related mineral stability diagrams. *ACS Sustainable Chem. Eng.* **2020**, *8*, 6647−6656.

(26) Pan, S.-Y.; Hung, C.-H.; Chan, Y.-W.; Kim, H.; Li, P.; Chiang, P.-C. Integrated CO_2 fixation, waste stabilization, and product utilization via high-gravity carbonation process exemplified by circular fluidized bed fly ash. *ACS Sustainable Chem. Eng.* **2016**, *4*, 3045−3052.

(27) Shuto, D.; Igarashi, K.; Nagasawa, H.; Iizuka, A.; Inoue, M.; Noguchi, M.; Yamasaki, A. CO_2 fixation process with waste cement powder via regeneration of alkali and acid by electrodialysis: Effect of Operation Conditions. *Ind. Eng. Chem. Res.* **2015**, *54*, 6569−6577.

(28) Ji, L.; Yu, H.; Li, K.; Grigore, M.; Yang, Q.; Wang, X.; Chen, Z.; Zeng, M.; Zhao, S.; et al. Integrated absorption-mineralisation for low-energy CO_2 capture and sequestration. *Appl. Energy* **2018**, *225*, 356−366.

(29) Ji, L.; Yu, H.; Yu, B.; Jiang, K.; Grigore, M.; Wang, X.; Zhao, S.; Li, K. Integrated absorption−mineralisation for energy-efficient CO_2 sequestration: Reaction mechanism and feasibility of using fly ash as a feedstock. *Chem. Eng. J.* **2018**, *352*, 151−162.

(30) Liu, M.; Gadikota, G. Integrated CO_2 capture, conversion, and storage to produce calcium carbonate using an amine looping strategy. *Energy Fuels* **2019**, *33*, 1722−1733.

(31) Liu, M.; Asgar, H.; Seifert, S.; Gadikota, G. Novel aqueous amine looping approach for the direct capture, conversion and storage of CO_2 to produce magnesium carbonate. *Sustainable Energy Fuels* **2020**, *4*, 1265−1275.

(32) Iizuka, A.; Yamasaki, A.; Honma, M.; Hayakawa, Y.; Yanagisawa, Y. Aqueous Mineral Carbonation Process via Concrete Sludge. *Kagaku Kougaku Ronbunshu* **2012**, *38*, 129.

(33) Iizuka, A.; Sakai, Y.; Yamasaki, A.; Honma, M.; Hayakawa, Y.; Yanagisawa, Y. Bench-scale operation of a concrete sludge recycling plant. *Ind. Eng. Chem. Res.* **2012**, *51*, 6099−6104.

(34) Iizuka, A.; Sakai, T.; Honma, M.; Yoshida, H.; Hayakawa, Y.; Yanagisawa, Y.; Yamasaki, A. Pilot-scale operation of a concrete sludge recycling plant and simultaneous production of calcium carbonate. *Chem. Eng. Commun.* **2017**, *204*, 79−85.

(35) Venhuis, M. A.; Reardon, E. J. Vacuum Method for Carbonation of Cementitious Wasteforms. *Environ. Sci. Technol.* **2001**, *35*, 4120−4125.

(36) Šavija, B.; Luković, M. Carbonation of cement paste: Understanding, challenges, and opportunities. *Constr. Build. Mater.* **2016**, *117*, 285−301.

(37) Lippiatt, N.; Ling, T.-C.; Pan, S.-Y. Towards carbon-neutral construction materials: Carbonation of cement-based materials and the future perspective. *J. Build. Eng.* **2020**, *28*, No. 101062.

(38) Chen, T.; Gao, X.; Qin, L. Mathematical modeling of accelerated carbonation curing of Portland cement paste at early age. *Cem. Concr. Res.* **2019**, *120*, 187−197.

(39) Chen, T.; Gao, X. Effect of carbonation curing regime on strength and microstructure of Portland cement paste. *J. CO$_2$ Util.* **2019**, *34*, 74−86.

(40) Zhan, B. J.; Xuan, D. X.; Poon, C. S.; Shi, C. J. Mechanism for rapid hardening of cement pastes under coupled CO$_2$-water curing regime. *Cem. Concr. Compos.* **2019**, *97*, 78−88.

(41) Shao, Y.; Roatami, V.; He, Z.; Boyd, A. J. Accelerated carbonation of Portland limestone cement. *J. Mater. Civ. Eng.* **2014**, *26*, 117−124.

(42) Tu, Z.; Guo, M.-Z.; Poon, C. S.; Shi, C. Effects of limestone powder on CaCO$_3$ precipitation in CO$_2$ cured cement pastes. *Cem. Concr. Compos.* **2016**, *72*, 9−16.

(43) Qin, L.; Gao, X. Recycling of waste autoclaved aerated concrete powder in Portland cement by accelerated carbonation. *Waste Manage.* **2019**, *89*, 254−264.

(44) Lilkov, V.; Petrov, O.; Kovacheva, D.; Rostovsky, I.; Tzvetanova, Y.; Petkova, V.; Petrova, N. Carbonation process in cement with mineral additions of natural zeolite and silica fume−Early hydration period (minutes) up to 24 hours. *Constr. Build. Mater.* **2016**, *124*, 838−845.